A closed-cycle dilution refrigerator for space applications

Gunaranjan Chaudhry[1], Angela Volpe[1], Philippe Camus[1], Sebastian Triqueneaux[2] and Gerard Vermeulen[1]

[1] *Institut Néel, CNRS-Universite Joseph Fourier, BP 166, F-38042 Grenoble Cedex 9, France*

[2] *Air Liquide DTA, 2 chemin de Clémencière, 38360 Sassenage, France*

Abstract

We discuss the development of a gravity-insensitive dilution refrigerator adapted from the open-cycle refrigerator used for the Planck mission. Since the ^{3}He and ^{4}He components are circulated (the ^{4}He by a fountain-effect pump operating at about 2 K, the ^{3}He by a compressor at room temperature) rather than ejected into space, the lifetime of a closed-cycle refrigerator is not limited by the quantity of ^{3}He and ^{4}He available. In this work, we concentrate on the design and performance of the cold end (counterflow heat exchanger and mixing chamber) of the refrigerator. We discuss the sizing of the heat exchanger and present cooling power measurements. We detail the working of the fountain pump. We also briefly touch upon some practical issues including the choice of a ^{3}He compressor and the pre-cooling requirements for the dilution refrigerator.

Keywords: Dilution refrigerator; Space cryogenics

1. Introduction

Conventional dilution refrigerators are commonly used to cool down to temperatures well below 100 mK. However, they require gravity for their operation and cannot be used for space applications. The High-Frequency Instrument aboard the Planck satellite was cooled by a dilution refrigerator [1] different from regular terrestrial ones. The "open-cycle" dilution refrigerator (OCDR) on the Planck satellite operates by flowing both ^{3}He and ^{4}He from separate reservoirs, mixing them to provide cooling and ejecting the mixture into space. This design works in zero-gravity since (a) the mixing process does not require gravity to separate the concentrated and dilute phases in the mixing chamber, and (b) the still, which requires gravity to separate the liquid and vapour phases, is completely eliminated. The lifetime of this fridge is obviously limited by the amount of ^{3}He and ^{4}He that can be carried in the reservoirs. The lifetime of the OCDR aboard Planck was about two years. This fridge provided 0.1 µW of cooling at 100 mK.

Instruments aboard future space missions such as SPICA and IXO/ATHENA require higher cooling powers at lower temperatures - 1 µW at about 50 mK [2]. These missions are also projected to have longer operating times of about 5 years. These conditions render the OCDR impractical - the amount of ^{3}He and ^{4}He required is simply too large to store on the satellite and to buy given current price and availability. This has driven the development of a new gravity-independent dilution refrigerator in which the mixture is not ejected into space but separated out into its components which are then cycled back. A schematic of this system is shown in Fig.1. The low-temperature part of the fridge (the counterflow heat exchanger, the mixing chamber and the load heater) is much the same as in the OCDR, although it must be significantly more effective than the Planck OCDR since the fridge is provisionally being designed to provide 1 µW of cooling at 50 mK. The major difference, however, between this fridge and the OCDR is the addition of the ^{3}He-^{4}He separation/circulation system. The returning mixture enters the still where the two components are separated. A bifilar spiralled heater in the still vaporizes nearly-pure ^{3}He which is circulated by a room temperature compressor. The ^{4}He liquid in the still flows through a superleak and is circulated by a fountain effect pump operating at about 2 K. The cycled ^{3}He and ^{4}He are cooled first in a 1.7 K thermal reservoir and then in the still before making their way down the counterflow heat exchanger. The mixing chamber is a Y-junction of the three capillaries forming the heat exchanger, so that capillary forces separate the concentrated phase from the dilute phase, instead of gravity.

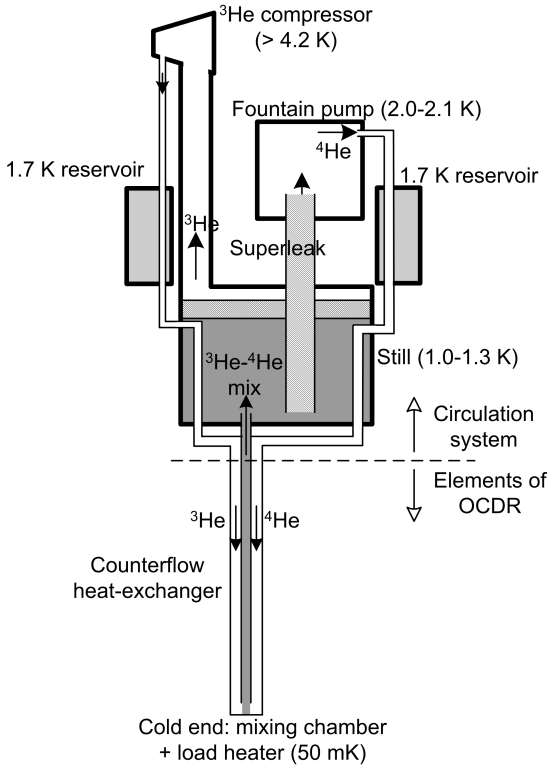

Figure 1: A schematic of the closed-cycle gravity-independent dilution refrigerator.

Preliminary results from a prototype have previously been presented [3]. In this paper, we discuss the advances made since then. We discuss the low-temperature part in detail including counterflow heat exchanger designs. We discuss the fountain pump which circulates the ^{4}He, and the requirements for a ^{3}He compressor. We briefy discuss the integration of the fridge in a cooling chain and calculate its pre-cooling requirements.

Before we proceed, we should point out that all the testing to date has been done with a regular still requiring gravity. Currently, the focus of research is on the development of a gravity-independent still using capillarity to confine the liquid inside a metal sinter.

2. Low-temperature part of the fridge

The low-temperature part of the fridge consists of the counterflow heat exchanger, the mixing chamber and the load heater. Two different counterflow heat exchanger designs were considered. The first design (Fig. 2a) is identical to that used in the Planck OCDR (other than having larger dimensions). Three sets of Cu-Ni capillaries soldered together form the flow passages for the two hot streams (pure ^{3}He and pure ^{4}He) and the cold stream (^{3}He-^{4}He mixture). The heat exchanger consists of a 1m-long "single-phase" section with 0.2 mm (inner diameter) capillaries and a 6m-long "two-phase" section with larger (0.4 mm and 0.6 mm capillaries). Martin et al. [3] discuss in more detail the reasons for this design: it ensures that the mixture flows at constant concentration x rather than at constant ^{4}He chemical potential μ_4. (This is required to ensure that the concentration in the still is much higher than in a conventional dilution refrigerator, in order that the still pressure be within the range of a reasonably-sized ^{3}He compressor.) At lower temperatures, the returning mixture is typically two-phase and the normal concentrated phase breaks the continuity of μ_4 by preventing the superfluid in the dilute phase from flowing freely. At higher temperatures when the mixture becomes single-phase, the small capillary size drives the flow velocity above the critical velocity beyond which the normal and superfluid components are locked together.

In the second design (Fig. 2b), the ^{4}He capillaries are replaced by a superleak. The ^{3}He and mixture capillaries are identical to those in the first design. This design was driven by experiments on the first design which suggested that ^{3}He diffusing up the ^{4}He capillary was causing heating, presumably due to mutual friction, which was putting an extra heat load on the heat exchanger. The superleak is thermally

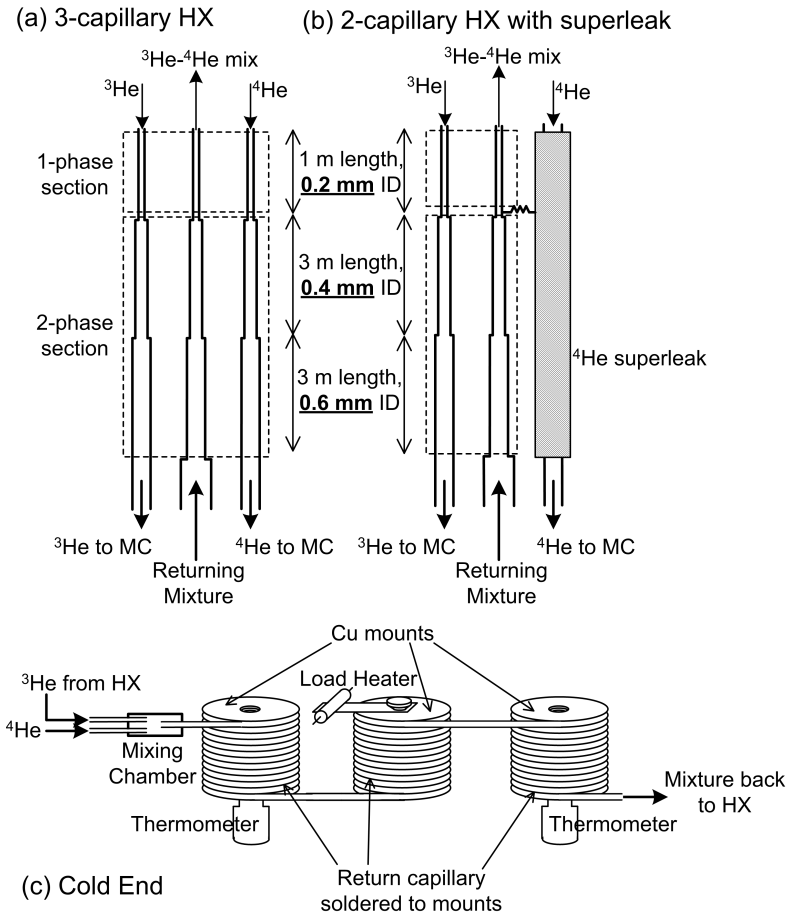

Figure 2: (a), (b) The two counterflow heat-exchanger designs tested. (c) The cold end of the fridge (not to scale), used with both heat exchangers. (MC: Mixing chamber, HX: Heat exchanger.) The thermometer on the left measures the mixing chamber temperature; the thermometer on the right measures the temperature of the mixture after absorbing the heat load, T_{load}.

isolated from the heat exchanger except for a single thermal short to prevent a conduction heat leak from the still to the mixing chamber.

The cold end of the fridge consists of a mixing chamber and a load heater. A schematic of the cold end is shown in Fig. 2c. The ^{3}He and ^{4}He capillaries enter the mixing chamber where they are mixed together. The mixture flows out of the mixing chamber through a return capillary. The return capillary is soldered to three copper mounts. A 50 cm length of return capillary is soldered onto each mount. The thermometer on the first mount measures the temperature of the mixture exiting the mixing chamber. The resistance heater on the second mount acts as the load heater. The thermometer on the third mount measures the temperature of the mixture after it has absorbed the load, T_{load}. After the third mount, the mixture returns to the heat exchanger.

2.1. Experimentation

2.1.1. Comparison of heat exchanger configurations

The first series of tests was a comparison of the two heat exchanger designs. Both designs were tested under the same operating conditions (still temperature, ^{3}He flow rate, ^{4}He flow rate and cooling load) and the resulting load temperatures T_{load} compared. Results showed that there was not much to choose between the two. The 2-capillary design performed only marginally better: for the same set of parameters, T_{load} for the 2-capillary design was typically about 1-2 mK lower than T_{load} for the 3-capillary design. There were indications of mutual-friction-induced-heating in the ^{4}He capillary in the 3-capillary heat exchanger: (a) the temperature profiles were significantly lower for the 2-capillary design than for the 3-capillary (Fig. 3), and (b) in the 3-capillary design, the temperatures of the ^{4}He stream were much

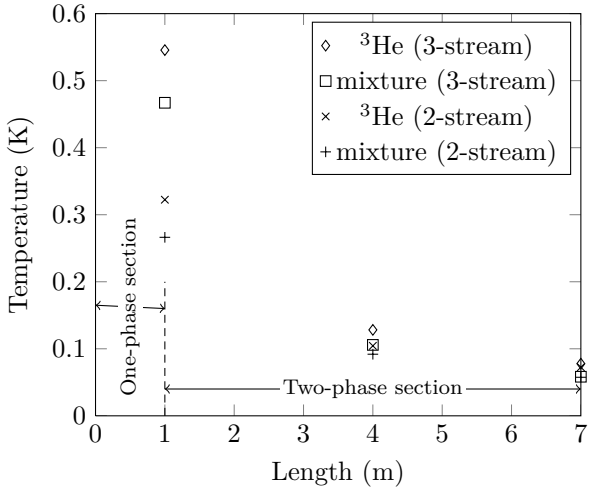

Figure 3: Experimental temperature profiles for the 3-capillary and 2-capillary heat exchangers under nearly identical operating conditions: T_{still} = 1.08 K, $\dot{n}_3 \approx 24$ µmol/s, $\dot{n}_4 \approx 320$ µmol/s, $\dot{Q}_{load}$=1 µW. The ^{3}He (and the ^{4}He in the 3-capillary exchanger) enter at T_{still} in both cases. Although not shown in this figure, the temperature of the ^{4}He stream is much higher than the corresponding temperatures of the ^{3}He and mixture streams in the 3-capillary exchanger.

higher than the corresponding temperatures of the ^{3}He stream. However, since the ultimate T_{load}'s for the two configurations were very close, it appears that there was enough exchange area in the 3-capillary design to compensate for the heating.

Since the 2-capillary design performed slightly better, most of the subsequent experiments were done using this configuration. All discussion from this point on is limited to the 2-capillary design.

2.1.2. Sizing of the cold end (return capillary)

After deciding to concentrate on the 2-capillary design, efforts turned to optimising the performance of the fridge. Early experiments showed a cooling power of 1 µW at a T_{load} of about 55 mK in the best case [3]. In these experiments, the return capillary had an inner diameter of 0.6 mm. It was observed that with this capillary, there was nearly a 5 mK temperature rise over a 1 m (adiabatic) length in the absence of any applied heat load. (This was the temperature rise between the two thermometers in Fig. 2c with the load heater turned off.) It was clear that this detracted significantly from the performance of the fridge. Since there were no other apparent sources of a heat leak, viscous heating in the return capillary was suspected to be the cause. The theoretical temperature rise per unit length due to viscous heating is [4]:

$$\frac{\Delta T}{\Delta x} \approx \frac{128\eta}{\pi D^4 c}\dot{n}v^2 \tag{1}$$

where $\dot{n}$ is the flow rate, c the specific heat, η the viscosity and v the molar volume of the mixture, and D the inner diameter of the return capillary. The calculation yields a temperature rise per unit length of about 4 mK per metre, in good agreement with experiment. Since the viscous temperature rise is proportional to the inverse of D^4, a return capillary diameter of 1 mm should produce a $\Delta T_{viscous}$ only about an eighth of that with a 0.6 mm capillary, i.e., about 0.5 mK. Therefore a return capillary size of 1 mm was chosen for subsequent experiments. This had the predicted effect and significantly improved performance. T_{load} decreased from about 55 mK at 1 µW to about 45 mK at 1 µW.

A theoretical analysis of the heat exchanger capillaries [4] showed that there were no major improvements to be had by increasing the sizes of those capillaries - they were already big enough for viscous dissipation not to be a limiting factor. Of course, one of the reasons that the return capillary size is more critical is that the viscosity scales with T^{-2} and therefore is more of an issue at the lowest temperatures.

Table 1: The minimum load temperatures achieved with a 1 μW heat load at various still pressures. The effect of the ^{3}He flow fraction (x_{app}) on the cooling power of the fridge is discussed in the text.

P_{still} (mbar)	T_{still} (mK)	Flow rate of still vapour circulated by compressor (mostly ^{3}He) $\dot{n}_v$ (μmol/s)	Fraction of ^{3}He in still vapour (x_v) [5]	Flow rate circulated by fountain pump $\dot{n}_{FP}$ (all ^{4}He) (μmol/s)	Flow fraction of ^{3}He in the mixture, $x_{app} = \frac{\dot{n}_3}{\dot{n}_3+\dot{n}_4} = \frac{x_v \dot{n}_v}{\dot{n}_v+\dot{n}_{FP}}$	T_{load} (mK)
0.4	0.7 K	16.6	1	392.6	0.041	44.0
5.0	1.1 K	18.5	0.96	348.8	0.048	45.0
10.0	1.3 K	28.8	0.85	340.2	0.066	46.7
15.0	1.5 K	57.0	0.75	300.3	0.119	51.8

2.1.3. Effect of still pressure on fridge performance

As mentioned earlier, it is desirable that the still pressure P_{still} be as high as possible so as to ease the requirements on the ^{3}He compressor. However, the performance of the fridge worsens as the still pressure increases. A high still pressure corresponds to a high still temperature which raises the temperature of ^{3}He stream entering the counterflow heat exchanger, ultimately resulting in a higher T_{load}. Experiments were done at various still pressures to find the highest values of P_{still} at which the fridge would still be able to produce 1 µW of cooling at temperatures below 50 mK.

The performance of the fridge at various still pressures is tabulated in Table 1. We tested our system at still pressures of up to 15 mbar. T_{load} was obviously lowest when the still pressure was at its lowest value of about 0.4 mbar. When the still pressure was increased from 0.4 to 5.0 mbar, T_{load} increased by less than 1 mK. When the still pressure was raised to 10 mbar, T_{load} increased by 2 mK to about 47 mK. Finally, when the still pressure was increased to 15 mbar, T_{load} increased significantly to about 52 mK. These numbers suggest that a still pressure of 10 mbar is quite acceptable for this system. However, the fridge is not good enough at present to achieve the target T_{load} of 50 mK with a still pressure of 15 mbar. Improvements are required to make a 15 mbar still viable; one possibility is an increase in the length of the heat exchanger for more exchange area and therefore more effective pre-cooling.

2.1.4. Cooling power of the fridge

The fridge was also tested at various heat loads. T_{load} is plotted as a function of the heat load in Fig. 4. For load temperatures below 150 mK, the heat load (i.e., the cooling power) approximately follows the relation (Fig. 4):

$$\dot{Q}_{load} \approx 2.6 \dot{n}_4 T_{load}^2 \tag{2}$$

which is in good agreement with the theoretical relation [4]:

$$\dot{Q}_{load} \approx 3 \dot{n}_4 T_{load}^2 \tag{3}$$

2.1.5. Effect of flow rates

The effects of varying the flow rates of the ^{4}He and ^{3}He components were also studied. The ^{4}He flow rate was generally kept at the maximum allowed by the fountain pump (discussed in the following section), typically between 300-400 µmol/s, depending on P_{still}. A higher flow rate implies a higher cooling power, as long as it is low enough for viscous dissipation to not be a major concern. With our heat exchanger and return capillary sizing, it wasn't.

The ^{3}He flow rate is a critical parameter. Below a certain flow fraction ($x_{app} = \frac{\dot{n}_3}{\dot{n}_3+\dot{n}_4}$), the fridge does not cool. (Note that x_{app} is the averaged concentration of the overall mixture if the mixture happens to be two-phase.) Although it had previously been believed [6] that the only requirement for cooling was that x_{app} be greater than the limiting concentration of 6.6% (i.e., the mixture be two-phase in the mixing

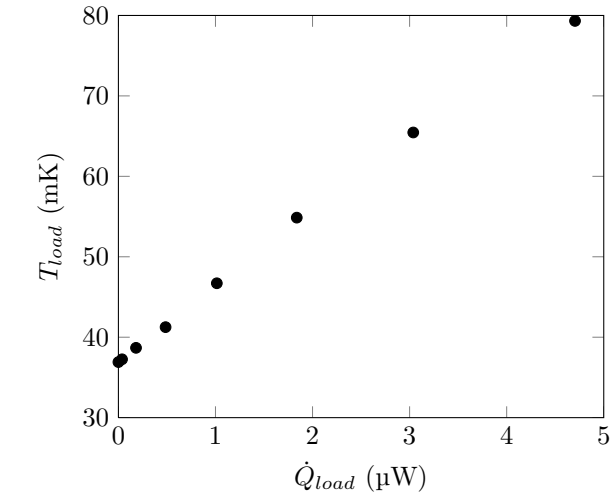

(a) T_{load} vs $\dot{Q}_{load}$

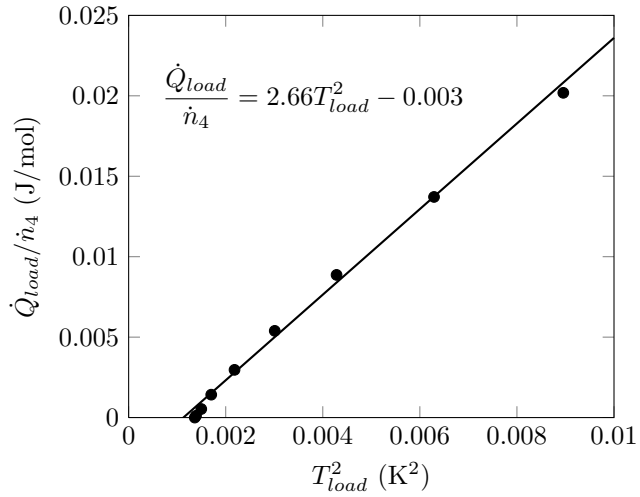

(b) $\dot{Q}_{load}/\dot{n}_4$ vs T_{load}^2

Figure 4: Experimental cooling power data at a still pressure of 10 mbar: (a) the load temperature as a function of the cooling power, and (b) the specific cooling power as a function of T_{load}^2 (data - squares, fit - solid line) for the same data. Load temperatures of less than 50 mK are achievable at 1 µW of cooling power. Even though T_{load} appears to be linear with $\dot{Q}_{load}$ over the small scales in (a), $\dot{Q}_{load}$ actually scales approximately with T_{load}^2 at low temperatures since the enthalpies of the mixture and of pure ^{3}He scale with T^2 at low temperatures.

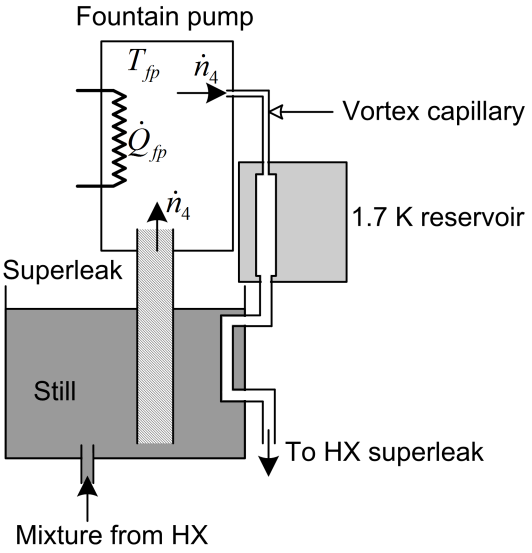

Figure 5: The fountain pump and the ^{4}He circulation loop. Superfluid ^{4}He flows through the superleak from the still into the fountain pump, drawn by the fountain effect. A heat input $\dot{Q}_{fp}$ is applied to the fountain pump. Bulk ^{4}He flows out of the fountain pump and is cooled, first in the 1.7 K reservoir and then in the still, before making its way down the heat exchanger.

chamber), it appears that this theory is too simplistic. The minimum required flow fraction increases with P_{still}. At the lowest values of P_{still}, cooling is observed with x_{app}'s of less than 6.6%. At the highest values of P_{still}, the minimum x_{app} needs to be much greater than 6.6% for cooling to occur. (The results in Table 1 are all at the minimum x_{app} for the corresponding P_{still}.) It is possible that x_{app} is different from the local mixture concentration which is what actually decides whether the mixture is single-phase or two-phase.

2.1.6. Summary

The present configuration of the low-temperature part of the fridge is capable of delivering 1 µW of cooling power at temperatures below 50 mK at still pressures of up to 10 mbar. The performance of the heat exchanger and the cold end is in reasonable agreement with models. Typical flow rates required for the 1 µW cooling power are about 20-30 µmol/s for ^{3}He and 300-400 µmol/s for ^{4}He, with higher ^{3}He flow fractions required at higher still pressures. In the following section, we discuss the fountain pump used to circulate the ^{4}He.

3. Fountain pump

The fountain pump is used to circulate the ^{4}He component through the refrigerator. A schematic is shown in Fig. 5. The fountain pump box is connected to the still through a superleak. A heater heats the ^{4}He in the pump, and ^{4}He is drawn from the still through the superleak into the pump by means of the fountain effect. The ^{4}He flows from the fountain pump through the vortex capillary to the 1.7 K reservoir where it is cooled. The diameter of the vortex capillary is chosen so that the flow under typical operating conditions is highly turbulent. In this case, the superfluid component is locked to the normal component and all the heat applied to the fountain pump goes into driving the flow. The ^{4}He is further cooled in the still, down to the still temperature, and then flows down to the mixing chamber.

Since the ^{4}He flow rate is a critical parameter in the operation of the fridge - the cooling power of the fridge scales with the ^{4}He flow rate - it is worth understanding the factors that affect it. The ^{4}He flow rate induced by the pump can be calculated by applying the Second Law to a control volume consisting of the fountain pump box in Fig. 5. At steady state and with no entropy generation:

$$0 = \frac{\dot{Q}_{fp}}{T_{fp}} + \dot{n}_4 s_{4,in} - \dot{n}_4 s_{4,out} \tag{4}$$

where $s_{4,in}$ is the entropy of the ^{4}He superfluid entering the pump (and is equal to zero, since the superfluid carries no entropy) and $s_{4,out}$ is the entropy of ^{4}He at the temperature of the fountain pump, T_{fp}. $\dot{Q}_{fp}$ is the heat input applied to the fountain pump via a resistance heater. The external heat conduction from the fountain pump was measured to be negligibly small; therefore $\dot{Q}_{fp}$ is the only heat transfer process across the fountain pump control volume. As the ^{4}He can be modelled as an incompressible liquid, its entropy may be assumed to be a function of only its temperature and not of its pressure. Therefore the heat input is related to the ^{4}He flow rate $\dot{n}_4$ by

$$\dot{Q}_{fp} = \dot{n}_4 T_{fp} s_4(T_{fp}) \tag{5}$$

A critical heat input is required to induce bulk ^{4}He flow. At heat inputs below the critical value, the thermal counterflow of ^{4}He between the fountain pump and the 1.7 K reservoir is sufficient to remove all the heat without bulk flow. This critical heat input (the maximum heat that can be transferred by counterflow with mutual friction between the normal and superfluid components) is calculated from [7]:

$$\dot{Q}_{crit} = A \left(\frac{\rho^2 s_\lambda^4 T_\lambda^3}{L A_\lambda} \int_{T_{res}}^{T_{fp}} \left(\left(\frac{T}{T_\lambda} \right)^{5.7} \left(1 - \left(\frac{T}{T_\lambda} \right)^{5.7} \right) \right)^3 dT \right)^{1/m} \tag{6}$$

where L and A are the length and the cross-sectional area of the vortex capillary between the fountain pump and the 1.7 K reservoir, ρ is the density of ^{4}He (145 kg/m^3), s_λ is the specific entropy of ^{4}He at T_λ (1559 J/kgK), A_λ is the Gorter-Mellink coefficient at T_λ (1450 m-s/kg) and m is approximately 3. For the capillary between the fountain pump and the 1.7 K reservoir (72 µm diameter, 0.12 m length), $\dot{Q}_{crit}$ is calculated to be about 0.13 mW for $T_{fp} = 2.1$ K and $T_{res} = 1.7$ K. However, the experimental value of the critical heat load was higher at about 0.2-0.24 mW.

The bulk flow rate that can be induced (by applying $\dot{Q}_{fp} > \dot{Q}_{crit}$) is limited by the restriction that the fountain pump temperature T_{fp} be less than the λ-temperature of ^{4}He, $T_\lambda = 2.176$ K at saturated pressure. Eq. 5 does not impose a limit on the flow rate; it is possible in theory to increase $\dot{n}_4$ by increasing $\dot{Q}_{fp}$ while keeping T_{fp} constant. This is not the case in practice, however. As $\dot{n}_4$ increases, the pressure drop in the ^{4}He flow passages increases. The increase in pressure drop results in a rise in the fountain pump pressure P_{fp} and a corresponding rise in T_{fp}. Therefore, the pressure drop limits the maximum flow rate through the system. To show this, we first consider the pressure balance across the ^{4}He flow passages (from the fountain pump to the 1.7 K reservoir, to the still, to the mixing chamber, and back up the mixture capillary to the still):

$$P_{fp} - P_{still} \approx \Delta P \tag{7}$$

where ΔP is the pressure drop in the flow capillaries, P_{fp} is the fountain pump pressure and P_{still} is the still pressure. In addition, the equivalence of the ^{4}He chemical potential across the superleak between the still and the fountain pump yields (keeping in mind that the fountain pressure at T_{still} is much less than that at T_{fp}):

$$P_{fp} - P_f(T_{fp}) \approx P_{still} - \Pi(T_{still}, x_{still}, P_{still}) \tag{8}$$

where $P_f(T_{fp})$ is the fountain pressure of ^{4}He at the fountain pump temperature T_{fp}, Π is the osmotic pressure in the still and x_{still} is the ^{3}He concentration in the still. The above equations give:

$$P_f(T_{fp}) \approx \Pi(T_{still}, x_{still}) + \Delta P \tag{9}$$

This shows why T_{fp} increases with $\dot{n}_4$: since ΔP increases with $\dot{n}_4$, $P_f(T_{fp})$ and thus T_{fp} increase with $\dot{n}_4$ (for the same still conditions). Therefore, as $\dot{Q}_{fp}$ is increased in an attempt to raise the flow rate, T_{fp} also rises.

We now take a closer look at the dependence of ΔP, and therefore $P_f(T_{fp})$, on the flow rate. In the flow passages in our system, the major pressure drop occurs in the 72 µm diameter vortex capillary between

the fountain pump and the 1.7 K reservoir. The pressure drop is related to the flow rate through the formula:

$$\Delta P = f\frac{L}{d}\frac{\rho}{2}\left(\frac{\dot{n}_4 M_4}{\rho\frac{\pi d^2}{4}}\right)^2 \tag{10}$$

where f is the friction factor, L the length and d the diameter of the capillary, ρ the density and M_4 the molecular mass of ^{4}He. (The term inside the brackets is the velocity of the fluid.). The transition between laminar and turbulent flow occurs at Reynolds numbers of the order of 2000. This corresponds to a ^{4}He flow rate through the 72 µm capillary of about 50 µmol/s. We are always over this value. For turbulent flow, the friction factor is $f_{turb} = 0.316Re_d^{-1/4}$[8], where the Reynolds number Re_d is based on the viscosity of the normal fluid. Substituting the friction factor equation into the pressure drop expression, we get:

$$\Delta P_{turb} = 0.241L\left(\frac{\eta M_4^7 \dot{n}_4^7}{\rho^4 d^{19}}\right)^{1/4} \tag{11}$$

Plugging this pressure drop expression into Eq. 9, we get:

$$P_f(T_{fp}) \approx \Pi(T_{still}, x_{still}) + \left(\frac{0.241L\eta^{1/4}M_4^{7/4}}{\rho d^{19/4}}\right)\dot{n}_4^{7/4} \tag{12}$$

This means that the fountain pressure $P_f(T_{fp})$ is proportional to $\dot{n}_4^{1.75}$. The proportionality constant, $0.241L\eta^{1/4}M_4^{7/4}\rho^{-1}d^{19/4}$, is 2.41 $\times$ 10^{10} Pa-s$^{1.75}$/mol$^{1.75}$ for the 72 µm capillary.

We now compare this model with measurements. Experimental measurements of $P_f(T_{fp})$ versus flow rate are shown in Fig. 6. Also shown are fits to the data. The fits were chosen to be of the form:

$$P_f(T_{fp}) = A + B\dot{n}_4^m \tag{13}$$

To calculate the fits, B was set equal to the theoretical value (2.41 $\times$ 10^{10} Pa-s$^{1.75}$/mol$^{1.75}$) and A and m calculated from the data. In theory, m should be equal to 1.75 and A, the y-intercept of the ΔP-$\dot{n}_4$ graph, should be equal to Π_{still}. The experimental values of m were really close to 1.75. The experimental values of A for the two data sets shown in Fig. 6 were (a) 295 mbar at P_{still} = 5 mbar, and (b) 142 mbar at P_{still} = 0.4 mbar. The corresponding still osmotic pressures for these cases, calculated from the still operating conditions and thermodynamic tables ([9] and [10]), were (a)Π_{still} = 324 mbar at P_{still} = 5 mbar, and (b) Π_{still} = 192 mbar at P_{still} = 0.4 mbar. Therefore, the data yields a functional dependence between T_{fp} and $\dot{n}_4$ that is consistent with Eq. 12; however, the data when extrapolated back to $\dot{n}_4$= 0 does not exactly give $P_f(T_{fp})_{(\dot{n}_4=0)} = \Pi_{still}$.

The ^{4}He flow rate as a function of fountain pump heat input is shown in Fig. 7 at two different still pressures. The maximum flow rates typically achieved (before T_{fp} hits the limit of 2.17 K) are of the order of 400 µmol/s which are sufficient to provide the 1 µW of cooling desired at 50 mK. Typical operational heat inputs are 3-3.5 mW. These values are reasonably consistent with the fountain pump model relating the heat input to the flow rate (Eq. 5 + Eq. 12). The flow rate at a given $\dot{Q}_{fp}$ increases with decreasing still pressure, hardly surprising since $P_f(T_{fp})$ is lower for a lower Π_{still}. For the same $\dot{Q}_{fp}$ and a lower Π_{still}, T_{fp} is lower and therefore $\dot{n}_4$ is higher. This trend is apparent in Fig. 7.

The fountain pump model suggests that using a vortex capillary with a diameter larger than the present 72 µm should reduce the required heat input. The advantage of running the fountain pump with a lower $\dot{Q}_{fp}$ is that it reduces the heat load on the 1.7 K reservoir. Preliminary experiments with a 137 µm diameter vortex capillary indeed show $\dot{Q}_{fp}$ to be lower by a factor of 2 for the same flow rate when compared with the 72 µm diameter capillary.

Finally, one of the practical considerations for the fountain pump is whether it can be cold-started, i.e., whether it is possible to start circulating ^{4}He from a state where the entire fridge is at a more or less uniform temperature and the ^{3}He concentration is uniform throughout the fridge. Since $P_f(T_{fp})$ must be

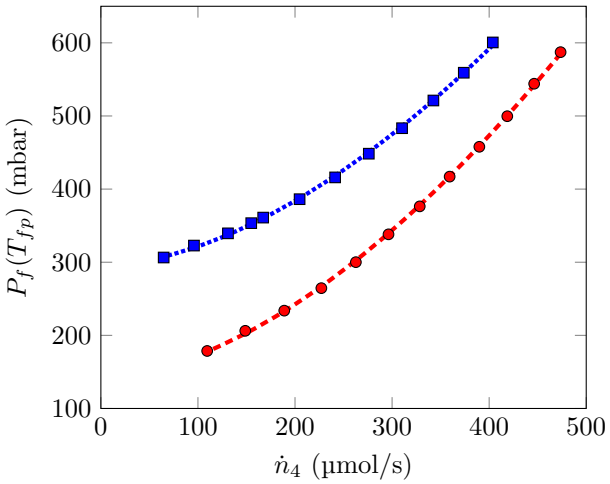

Figure 6: The ^{4}He fountain pressure at T_{fp} as a function of $\dot{n}_4$ at two still pressures: the upper data (blue squares) at P_{still} = 5 mbar, the lower data (red circles) at P_{still} = 0.4 mbar. The points are data; the curves are fits. The calculated exponents for the curves are 1.72 (0.4 mbar data) and 1.73 (5 mbar data), both quite close to the theoretical 1.75. The calculated y-intercepts for the curves are 142 mbar (0.4 mbar data) and 295 mbar (5 mbar data). All data are for x_{still}=0.1.

greater than Π_{still} for the ^{4}He to begin circulating, it is generally easier to start the fountain pump when the concentration of ^{3}He in the still is low, or when the temperature of the still is low. We observed during experiments that it was not always possible to start the fountain pump at a high still concentration and pressure. However, it was possible to operate it at those conditions by starting the fountain pump at a lower still pressure, and then increasing the pressure while it was still running. It is unclear what causes a difference between "operating" conditions and "start-up" conditions. This behaviour was observed only at very high concentrations ($x_{still} \approx 0.16$), where it was possible to operate the fountain pump at a still pressure of 5 mbar, but not cold-start the fountain pump beyond still pressures of 2.5 mbar. Importantly, though, at $x_{still} = 0.1$ (the concentration at which all the results in this paper are reported), it was possible to cold-start the fountain pump at still pressures as high as 15 mbar.

In summary, the present design of the fountain pump is capable of circulating enough ^{4}He to meet the cooling requirements of the fridge at present. It is also possible to start it up and operate it at still pressures of up to 15 mbar. The fountain pump model also suggests that it is possible to modify the ^{4}He flow loop (specifically, by increasing the size of the vortex capillary between the fountain pump and the 1.7 K reservoir) to decrease the operating temperature of the fountain pump thus reducing the heat load on the 1.7 K reservoir (discussed in the following section).

4. Integration of the refrigerator with the rest of the cooling chain

4.1. Choice of ^{3}He compressor

The ^{3}He compressor is an important component of the fridge. The fridge is currently at a stage of development where it can operate with a still pressure of 10 mbar and a flow rate of about 30 µmol/s. (A still pressure of 15 mbar may be workable in the future with a better counterflow heat exchanger but it currently provides 1 µW of cooling only at about 52-53 mK besides requiring a rather high flow rate of about 55 µmol/s for operation.)

The choice of a compressor is still an open question. At this point, three possibilities are being considered. One option is a sorption compressor similar in concept to the sorption compressor developed for the Darwin cooler at the University of Twente [11]. The sorption compressor for the dilution fridge will operate at about 15 K. The major challenge is the development of check valves that can work at low pressures - the check valves for the Darwin cooler work at 1 bar, while the dilution refrigerator requires valves that work at 0.2 bar. A second possibility being considered is a Holweck compressor [12], for which a test setup is being developed at Institut Neel, Grenoble. Besides these, a third option is the modification of a compressor being developed by the Japanese Space Agency JAXA for a ^{3}He J-T cooler for SPICA.

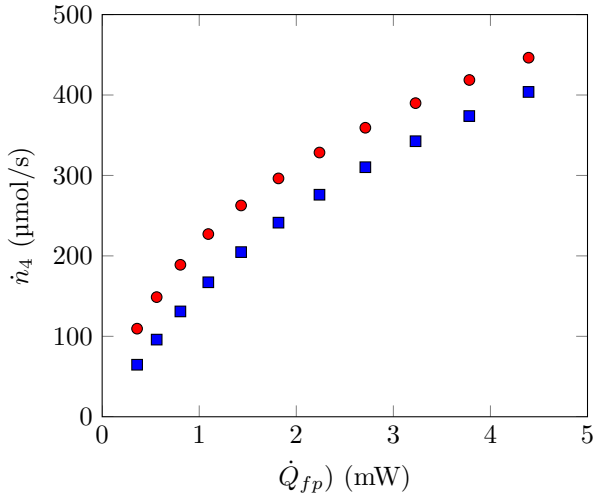

(a) $\dot{n}_4$vs $\dot{Q}_{fp}$

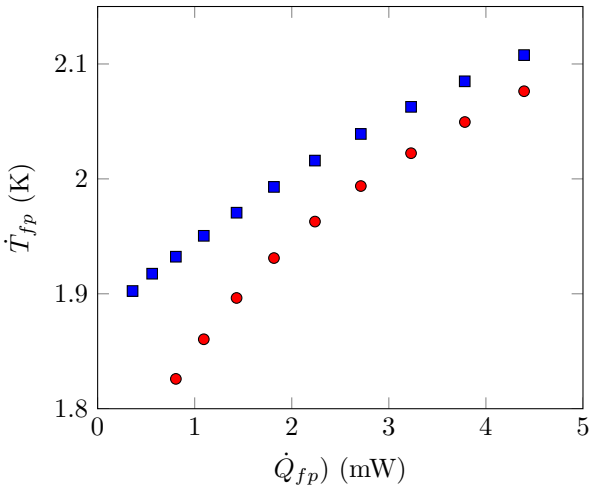

(b) T_{fp} vs $\dot{Q}_{fp}$

Figure 7: The ^{4}He flow rate and T_{fp} as a function of $\dot{Q}_{fp}$ at still pressures of 0.4 and 5.0 mbar (red circles: P_{still}=0.4 mbar, blue squares: P_{still} = 5 mbar). T_{fp} is lower and $\dot{n}_4$ higher for the lower P_{still}. This is because the still osmotic and fountain pressures are lower when the still pressure is lower and consequently the fountain pressure does not need to be as high.

Table 2: The estimated heat loads on the 1.7 K reservoir for the experiments listed in Table 1

P_{still} (mbar)	T_{still} (K)	T_{load} (mK)	Compressor flow $\dot{n}_v$ (μmol/s)	^{3}He fraction in compressor flow (x_v)	Fountain pump flow $\dot{n}_{FP}$ (μmol/s)	T_{fp} (K)	Heat load on 1.7 K reservoir from compressor flow (mW)	Heat load on 1.7 K reservoir from fountain pump flow (mW)
0.4	0.7 K	44.0	16.6	1	392.6	2.012	1.61	1.76
5.0	1.1 K	45.0	18.5	0.96	348.8	2.050	1.82	1.85
10.0	1.3 K	46.7	28.8	0.85	340.2	2.092	2.99	2.18
15.0	1.5 K	51.8	57.0	0.75	300.3	2.121	6.19	2.20

4.2. Pre-cooling requirements for the dilution refrigerator

The fridge requires a thermal reservoir at a temperature of about 1.7 K to cool ^{3}He gas down from 4.2 K (and condense it) and to cool the ^{4}He exiting the fountain pump. The SPICA project has a ^{3}He Joule-Thompson expansion stage with a total nominal cooling power of 10 mW at 1.7 K [13] to be shared between two scientific instruments. Therefore, it provides a pre-cooling power of 5 mW at 1.7 K. In the following, we calculate the cooling requirements of the fridge based on a reservoir temperature of 1.7 K.

The heat load from the ^{4}He circulated by the fountain pump is simply

$$\dot{Q}_{4He} = \dot{n}_4 \left(h_4^0(T_{fp}) - h_4^0(T_{res}) \right) \tag{14}$$

The heat loads in various experimental runs (at different still pressures) are tabulated in Table 2.

The heat load from the compressor flow (mostly ^{3}He, but there may be a bit of ^{4}He depending on P_{still}) is a little more complicated. The vapour entering the reservoir is assumed to be at 4.2 K. It is cooled down from 4.2 K to its saturation temperature, condensed into a liquid, and then cooled down to the temperature of the reservoir. (One of the requirements of the design is that the saturation temperature of the vapour be above the temperature of the reservoir, so that the fluid leaving the reservoir is assuredly liquid and doesn't put an excessive heat load on the still.) The heat load is therefore

$$\dot{Q}_{4He} = \dot{n}_v \left(c_{p,v}(4.2K - T_{sat}) + L(T_{sat}) + c_{p,l}(T_{sat} - T_{res}) \right) \tag{15}$$

where L is the latent heat of the mixture and $c_{p,v}$ and $c_{p,l}$ are the specific heats of the vapour and liquid respectively. The temperature T_{sat} depends on the pressure and concentration of the stream as it passes through the reservoir. We make the simplifying assumption that $T_{sat} = T_{res}$. Therefore, we assume that vapour enters the reservoir and just completely liquefies in it. We approximate the constant-pressure specific heat of the vapour as that of an ideal gas. We also approximate the latent heat of the vapour mixture as $x_v L_3^0 + (1 - x_v) L_4^0$ where x_v is the ^{3}He concentration in the vapour and L_3^0 and L_4^0 are the latent heats of pure ^{3}He and pure ^{4}He - 44.8 and 91.9 J/mol at 1.7 K respectively. This approximation overestimates the actual latent heat of the system [14] and therefore the actual heat load on the reservoir.

The heat loads in various experimental runs are tabulated in Table 2 alongside the heat loads due to ^{4}He circulated by the fountain pump. While the values in the tables are based partly on theoretical calculations, they were largely in agreement with direct experimental measurements of the heat load (4-6 mW absorbed by a 1.6 K reservoir, depending on operating conditions). The results show that it is possible to operate the fridge with a pre-cooling requirement of much less than 5 mW at still pressures of 5 mbar and less. With a still pressure of 10 mbar, the pre-cooling requirement is only slightly greater than 5 mW and optimisation of the flow rates will likely bring it down. Operating the fountain pump at a lower temperature for the same flow rate (by optimising the size of the vortex capillary between the fountain pump and the reservoir, as mentioned in the previous section) will also reduce the heat load on the reservoir. Other improvements are possible, notably by using a counterflow heat exchanger for the ^{3}He stream between 1.7 K and 4.2 K, or by using the hot ^{3}He vapour from the 4.2 K stage to provide the heat input for the fountain pump. However, these are options only when the fridge is operating in steady-state and start-up will require the entire load to be absorbed by the thermal reservoir.

5. Conclusion

In its present configuration, the closed-cycle gravity-independent dilution refrigerator is capable of providing 1 µW of cooling at about 45 mK. The fountain pump that circulates the ^{4}He component is well-characterised; a compressor to circulate the ^{3}He component still needs to be settled upon. The pre-cooling requirements for the fridge are about 3.7 mW at 1.7 K. These numbers are contingent upon the development of a compressor which can work down to 5 mbar. With a 10 mbar compressor, the performance degrades slightly (1 µW of cooling at 46.7 mK, 5.2 mW precooling required at 1.7 K) but there is scope for improvement. Currently, the focus of research is on the localisation of the vapour-liquid interface in the still. This problem has to be solved to render the dilution refrigerator really gravity-independent.

6. Acknowledgements

This work was funded by the Centre National d'Études Spatiales and by the European Space Agency (through an ITI grant).

7. References

[1] S. Triqueneaux, L. Sentis, P. Camus, A. Benoit, and G. Guyot. Design and performance of the dilution cooler system for the Planck mission. *Cryogenics*, 46(4):288–297, 2006.

[2] W. Holmes, J.J. Bock, C. Matt Bradford, T.C.P. Chui, T.C. Koch, A.U. Lamborn, D. Moore, C.G. Paine, M.P. Thelen, and A. Yazzie. Sub-Kelvin cooler configuration study for the Background Limited Infrared Submillimeter Spectrometer BLISS on SPICA. *Cryogenics*, 50(9):516–521, 2010.

[3] F. Martin, G. Vermeulen, P. Camus, and A. Benoit. A closed cycle ^{3}He-^{4}He dilution refrigerator insensitive to gravity. *Cryogenics*, 50(9):623–627, 2010.

[4] G. Chaudhry, A. Volpe, P. Camus, S. Triqueneaux, and G. Vermeulen. Development of the cold end of a gravity-insensitive closed-cycle dilution refrigerator. *Accepted for publication in Advances in Cryogenic Engineering 57*, 2012.

[5] T.R. Roberts and B.K. Swartz. Excess Thermodynamic Properties of Liquid ^{3}He-^{4}He Mixtures. In *Helium Three, Proceedings of the Second Symposium on Liquid and Solid He*, pages 158–172. Ohio State University Press, 1960.

[6] Adriana Sirbi, Alain Benoit, M. Caussignac, and Serge Pujol. The performance of an open cycle dilution refrigerator. *Czechoslovak Journal of Physics*, 46:2799–2800, 1996.

[7] Steven W. Van Sciver. *Helium Cryogenics*, page 144. Plenum Press, 1986.

[8] F. M. White. *Fluid Mechanics, Fifth edition*, page 362. McGraw-Hill, 2003.

[9] G. Chaudhry and J. G. Brisson. Thermodynamic Properties of Liquid ^{3}He-^{4}He Mixtures Between 0.15 K and 1.8 K. *Journal of Low Temperature Physics*, 155(5):235–289, 2009.

[10] S. G. Sydoriak and T. R. Roberts. Vapor Pressures of ^{3}He-^{4}He Mixtures. *Physical Review*, 118(4):901, 1960.

[11] J. F. Burger, H. J. M. Ter Brake, H. J. Holland, R. J. Meijer, T. T. Veenstra, G. C. F. Venhorst, D. Lozano-Castello, M. Coesel, and A. Sirbi. Long-life vibration-free 4.5 K sorption cooler for space applications. *Review of scientific instruments*, 78:65102–65111, 2007.

[12] J.A. Bhatti, M.K. Aijazi, and A.Q. Khan. Design characteristics of molecular drag pumps. *Vacuum*, 60:213–219, 2001.

[13] H. Sugita, Y. Sato, T. Nakagawa, T. Yamawaki, H. Murakami, H. Matsuhara, M. Murakami, M. Takada, S. Takai, S. Yoshida, and K. Kanao. Cryogenic system design of the next generation infrared space telescope SPICA. *Cryogenics*, 50:566–571, 2010.

[14] R. Radebaugh. *Thermodynamic properties of ^{3}He-^{4}He mixtures with applications to dilution refrigerators*, page 48. NBS Technical Note 362, 1967.